Increased Expression of Autophagy Protein Beclin1 and LC3 in High-grade Hepatocellular Carcinoma and Metastatic Carcinoma

Jongmin Kim^{1,†}, Jong Man Kim^{2,†}, Seok Joo Hong¹, Jun Ho Park¹, Sun Young Park¹, Taeho Hwang³, Gwan-Su Yi³, Seong Hwan Kim⁴, Eun Yoon Cho⁵, Jae-Won Joh², Jin Young Park¹ & Dae Shick Kim⁵

¹CbsBioscience, Inc., 59-5 Jang-dong, Yuseong-gu, Daejeon 305-343, Korea ²Department of Surgery, Samsung Medical Center, Sungkyunkwan University School of Medicine, 50 Ilwon-dong, Gangnam-gu, Seoul 135-710, Korea ³Department of Bio and Brain Engineering, Korea Advanced Institute of Science and Technology, 335 Gwahangno, Yuseong-gu, Daejeon 305-701, Korea ⁴Laboratory of Chemical Genomics, Korea Research Institute of Chemical Technology, P.O. Box 107, Yuseong-gu, Daejeon 305-600, Korea ⁵Department of Pathology, Samsung Medical Center, Sungkyunkwan University School of Medicine, 50 Ilwon-dong, Gangnam-gu, Seoul 135-710, Korea [†]These authors contributed equally to this work Correspondence and requests for materials should be addressed to J.Y. Park (jonnypark@cbsbio.com), D.S. Kim (oncorkim@skku.edu)

Accepted 23 October 2009

Abstract

Autophagy is frequently activated in tumor cells treated with chemotherapy or irradiation; thus, regulation of autophagy represents a promising target for cancer therapy. However, the expression levels of autophagy proteins, Beclin1 and LC3, and their localization patterns in relation to mTOR pathway markers in patients with hepatocellular carcinoma has not been elucidated. Eighty-two tissue specimens (69 paraffinembedded tissues and 13 frozen tissues) were obtained from patients with hepatectomy and expression levels of Beclin1, LC3, mTOR, and phospho-mTOR were analyzed by immunohistochemistry and western blots. Immunohistochemical analysis of 26 dysplastic nodules, 39 hepatocellular carcinomas, and 4 metastatic adenocarcinomas revealed a grade-dependent increase of immunostaining between grade II and III hepatocellular carcinoma for LC3 (P=0.02), Beclin1 (P=0.06), and mTOR (P<0.01), and between grade I and II hepatocellular carcinoma for phospho-mTOR (P=0.05). A high proportion of positive immunostaining of autophagy and mTOR pathway markers was found in 18 grade III/IV hepatocellular carcinoma tissues (44-100%) and in 4 metastatic adenocarcinoma tissues (75-100%). Examining immunohistochemical staining scores revealed a strong correlation between mTOR and Beclin1 (R²=0.74) and intermediate correlations between LC3 and Beclin1 ($R^2=0.54$) as well as between LC3 and phospho-mTOR (R²= 0.56). Western blotting of 13 frozen hepatocellular carcinoma tissue specimens revealed a similar overall increase of LC3, Beclin1, and mTOR. This study demonstrated that Beclin1 and LC3 expression levels are increased in high-grade hepatocellular carcinoma and metastatic adenocarcinoma. Moreover, LC3 and phospho-mTOR showed different localization patterns, and increased autophagosome formation was observed in the tumor cells with LC3 positivity. Thus, autophagy is frequently activated in high-grade hepatocellular carcinoma, and regulation of the autophagy process may have diagnostic and therapeutic potential.

Keywords: Autophagy, LC3, Beclin1, mTOR, Hepatocellular carcinoma

Introduction

Autophagy is a genetically programmed, evolutionarily conserved lysosomal pathway of self-digestion¹. During the process of autophagy, portions of the cytosol, organelles or targeted cargo are sequestered in double membrane-bound vesicles (autophagosomes). This double-membrane structure is a definitive characteristic of autophagic vacuoles. Autophagosomes then undergo progressive fusion with endosomes and lysosomes, resulting in autolysosomes in which the inner membrane and the luminal content of the autophagic vacuoles are degraded by lysosomal enzymes. In response to starvation, cells degrade non-essential components and thereby generate the nutrients required for vital processes². Thus, the autophagy machinery is tightly controlled by other cellular nutrient sensors. For instance, autophagy is inhibited by the mammalian target of rapamycin (mTOR). mTOR functions by integrating extracellular signals (growth factors, mitogens

and hormones) with amino acid availability and intracellular energy status to control translation rates and additional metabolic processes³. Translational control through mTOR plays a major role in regulating gene expression crucial for cell growth and survival. As such, the PI3K/Akt/mTOR signaling pathway is intimately implicated in cancer development and progression⁴. Rapamycin and its analogues inhibit mTOR, which normally suppresses autophagy, and therefore activates the autophagic process. It is possible that at least some of the anti-tumor effect of mTOR inhibitors is mediated by stimulating the autophagy pathway⁵.

Autophagy was linked to cancer by Levine and colleagues through their pioneering work on the identification and characterization of the autophagy specific gene Beclin1, which was first identified as a novel Bcl-2 interacting protein with anti-apoptotic activity^{6,7}. Becn1 - / - mice die early in embryogenesis, indicating its critical role in the developmental process. A monoallelic loss of Beclin1 (Becn1 - /+) increases the incidence of cancer in model animals; thus, Beclin1 is considered to be a haploinsufficient tumor suppressor^{8,9}. Accordingly, a single allelic deletion of the Becn1 harboring region, chromosome 17q21, is frequently observed in breast, ovarian, and prostate cancers¹⁰. However, the knockdown of *Becn1* in human tumor cells significantly inhibits cell proliferation, indicating that propagating tumor cells would have to maintain some level of Beclin1 protein¹¹. Several cancer cell lines show surprising resistance to nutrient starvation¹², while some aggressive malignant tumors, such as pancreatic cancers, are clinically hypovascular and potentially require alternative energy sources¹³. It is suggested that autophagy may be one of the mechanisms that supports cancer cell survival during nutrient starvation¹⁴. A recent study demonstrated that a mammalian homologue of yeast ATG8, LC3, whose cleaved form is a general marker for autophagic membranes¹⁵, is upregulated in colorectoral cancer tissues¹⁶. Thus, whether autophagy represents a survival mechanism or contributes to cell death in tumor tissue remains controversial. It is likely that the role of autophagy in cancer depends on the tissue origin of cancer, the stage of cancer development, the stromal and nutritional environment, or the degree of differentiation^{17,18}.

The involvement of the autophagy process during hepatocellular carcinoma (HCC) progression remains to be elucidated. As a preliminary study, an LC3-positive HCC tissue specimen was examined via transmission electron microscopy. Cancer cells contained lipid bilayer structures encapsulating cytoplasmic organelles, a distinctive characteristic for autophagosomes (Figure 1). To gain further insight into the role of autophagy proteins during HCC progression, the expression levels

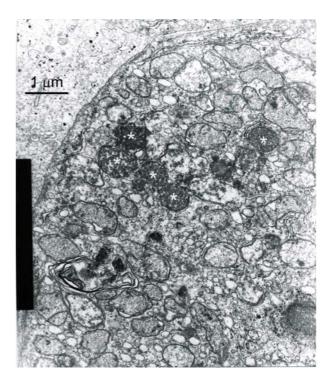


Figure 1. Ultrastructure of a HCC tissue in autophagy as shown by electron microscopy. Lipid bilayer structures engulfing organelles (*) are shown in the cytoplasm. Original magnification, \times 10,000.

and localization of Beclin1 and LC3 proteins were analyzed in 26 dysplastic nodule (DN), 39 HCC, and 4 metastatic adenocarcinoma formalin-fixed paraffinembedded (FFPE) tissue specimens using immunohistochemistry (IHC) along with 13 frozen HCC tissues examined by western blotting. In addition, the correlations between the expression levels of autophagy and mTOR pathway markers in patients with HCC were investigated using statistical analysis.

Results

Grade-dependent Expression Pattern of Beclin1 in HCC

Except for a low-grade DN and a high-grade DN that were stained weakly, none of the DNs were stained with Beclin1 antibody. In 39 primary HCC specimens, 27 specimens (69%) had a higher intensity of Beclin1 immunostaining in tumors compared with their adjacent, nontumor tissues (Figure 2). Low-grade HCC tissues showed weak and moderate Beclin1 immunopositivity in 44% of grade I and 42% of grade II HCC. However, grade III/IV HCC and metastatic adenocarcinoma showed 100% Beclin1 positivity; seven tissues (four grade III HCCs, one grade IV HCC, and two

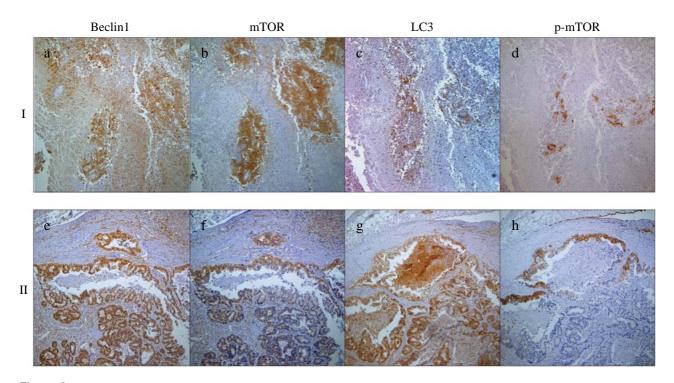


Figure 2. Expression of Beclin1, LC3, mTOR, and phosphorylated mTOR in Edmondson grade III HCC (I) and metastatic adenocarcinoma (II) tissues. (a, e) Grade III HCC and metastatic adenocarcinoma revealed a higher intensity of Beclin1 immunostaining compared with adjacent nontumor tissue (original magnification, \times 100). (b, f) Grade III HCC and metastatic adenocarcinoma revealed a higher intensity of mTOR immunostaining compared with adjacent nontumor tissue (original magnification, \times 100). (c, d, g, h) LC3 protein and phospho-mTOR (Ser2448) protein were detected with IHC using serial sections of paraffin-embedded grade III HCC and metastatic adenocarcinoma samples. LC3 and phospho-mTOR localized to different areas of cancerous tissue (original magnification, \times 100).

metastatic adenocarcinomas) showed strong positive staining for Beclin1 (Figure 3). Thus, Beclin1 showed HCC grade-dependent expression with relatively large differences in expression levels between high-grade DN and grade I HCC (P=0.07) as well as grade II and grade III HCC (P=0.06; Kruskal-Wallis rank sum test) (Table 1). A set of western blot experiments corroborated these results, in which 10 of the 13 paired tumor samples showed increased expression of Beclin1 proteins (Figure 4). Moreover, the average Beclin1 expression level was higher for grade III HCC compared to grade II HCC tissues, indicating potential relevance to tumor progression.

Increased LC3 Expression in High-grade HCC

Another important indicator of autophagy, LC3 expression, has not been investigated in primary HCC tissues. Therefore, the expression of LC3, whose cleaved form is regarded as an indicator of autophago-some formation¹⁵, was addressed by IHC. LC3-positive cells were not detected in 26 DNs. In 39 HCCs, 10 specimens (26%) showed a higher intensity of LC3

immunostaining in tumors compared with their adjacent, nontumor tissues (Figure 2). Except for one grade II HCC that was stained weakly, none of the grade I/II HCC specimens were stained with LC3 antibody, while 9 (50%) of 18 grade III/IV HCCs and 4 (100%) of 4 metastatic adenocarcinomas revealed moderate to strong LC3 staining (Figure 3). Thus, LC3 positivity showed HCC grade-dependence with significant differences in expression levels between grade II and grade III HCC (P=0.02) and grade IV HCC and metastatic adenocarcinoma (P=0.03; Kruskal-Wallis rank sum test) (Table 1). The expression of LC3 showed a positive correlation with Beclin1 expression in IHC intensity-sum scores calculated by multiplying the intensity score by the proportion score ($R^2=0.54$; Pearson's correlation). Interestingly, the proportions of LC3 positive cells were relatively small (typically 5%) in grade III/IV HCCs compared to Beclin1 positive cells. Close examination of the LC3-positive cells showed that the LC3 protein localized in the cytoplasm with irregular condensation in a manner similar to that of GFP-LC3 localization in autophagosome formation reported previously¹⁶. To investigate whether LC3 in

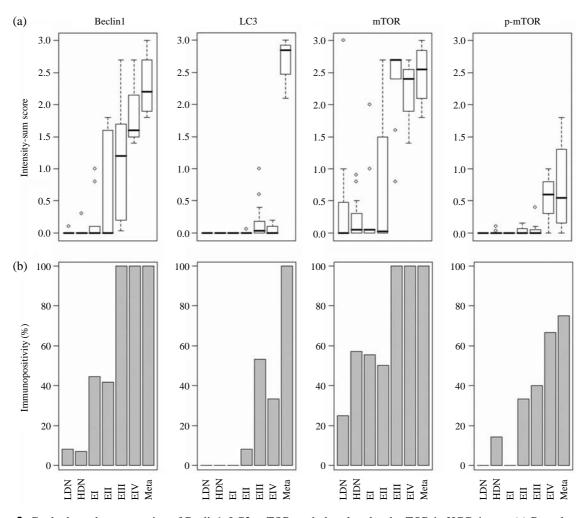


Figure 3. Grade-dependent expression of Beclin1, LC3, mTOR, and phosphorylated mTOR in HCC tissues. (a) Box plots showing the distribution of IHC intensity-sum scores by markers and grades. The ends of the box are the 25th and 75th percentiles of the scores. The median is shown as a solid line dividing the box. Lines (whiskers) extend from the ends of each box to the outermost data point lying within 1.5 times the length of the box. (b) Bar plots showing the percent immunopositivity by markers and grades. LDN, low-grade DN; HDN, high-grade DN; EI, Edmondson grade I HCC; EII, grade II HCC; EIII, grade III HCC; EIV, grade IV HCC; Meta, metastatic adenocarcinoma.

tumor tissues exist in a soluble form (LC3-I) or in a membrane-bound form (LC3-II), proteins extracted from frozen HCC tissues were probed for different isoforms of LC3 through western blotting. Eleven (85 %) of the 13 paired tumor samples showed increased expression of LC3-II proteins (Figure 4). Although LC3-II is closely correlated with the number of autophagosomes, LC3 immunoblotting is sometimes interpreted inappropriately due to its rapid turnover¹⁹. Thus, the LC3 ratio (LC3-II/LC3-I) could be used as a more reliable indicator of autophagy²⁰. Accordingly, 9 of the 11 HCC tissues with increased LC3-II expression showed an increased LC3 ratio (LC3-II/LC3-I), except for two cases in which the LC3-I increase was greater. These data suggest that autophagy machinery is active in high-grade HCC and may be relevant to the progression of tumors.

Expression Pattern of mTOR and Phospho-mTOR in HCC

Proteins regulating mTOR, as well as regulatory targets of mTOR kinase, are overexpressed in many cancers²¹, including HCC^{22,23}. Thus, mTOR and phosphomTOR expression profiles were analyzed and they were compared with the profiles of Beclin1 and LC3 expression in HCC. Eleven DNs (42.3%) were positively stained with mTOR antibody. Increased mTOR immunostaining was found in 29 HCCs (74%) compared with their adjacent, nontumor tissues (Figure 2). The proportion of mTOR immunopositivity was simi-

Table 1. Kruskal-Wallis rank sum test	statistics for mean intensity-sur	n score differences between HCC grades.

Grades	Low-grade DN	High-grade DN	Grade I HCC	Grade II HCC	Grade III HCC	Grade IV HCC	Metastatic adenocarcinoma
No. of samples	12	14	9	12	15	3	4
Beclin1		1	0.07	0.48	0.06	0.21	0.29
LC3		NA	NA	0.36	0.02	0.57	0.03
mTOR		0.46	0.62	0.86	< 0.01	0.48	0.47
p-mTOR		0.17	0.2	0.05	0.87	0.12	0.86

NA=not applicable

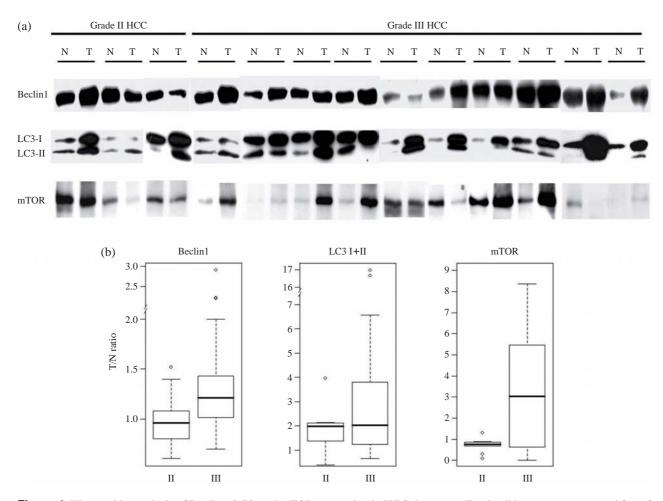


Figure 4. Western blot analysis of Beclin1, LC3, and mTOR expression in HCC tissues. (a) Total cell lysates were prepared from 3 grade II and 10 grade III HCC tissues and Beclin1, LC3, and mTOR were detected with Western blotting. Both LC3-I and LC3-II bands were detected by LC3 antibody. One representative blot out of three to four replicate experiments is shown for each marker. N, noncancerous tissue; T, HCC tissue. (b) Box plots showing the marker densities in grade II and grade III HCC tissues divided by marker densities in paired noncancerous tissues. For the box plot titled "LC3 I+II", the sum of the LC3 I and LC3 II band densities were compared for HCC tissues and paired noncancerous tissues. II, grade II HCC; III, grade III HCC.

lar for grade I (56%) and grade II HCC (50%), but the overall staining intensity was increased due to two strong positive cases in grade II HCC tissues. Furthermore, grade III/IV HCC and metastatic adenocarcinoma showed 100% mTOR positivity, in which seven-

teen tissues (twelve grade III HCCs, two grade IV HCCs, and three metastatic adenocarcinomas) showed strong positive staining for mTOR (Figure 3). Thus, mTOR expression showed HCC grade-dependence with a significant difference in expression levels bet-

ween grade II and grade III tissues (P<0.01; Kruskal-Wallis rank sum test) (Table 1). Interestingly, the expression of mTOR showed a strong correlation with Beclin1 expression ($R^2=0.74$; Pearson's correlation) in IHC intensity-sum scores, and their expression patterns largely overlapped (Figure 2). However, a weaker correlation was observed for mTOR expression and LC3 expression ($R^2=0.39$; Pearson's correlation). A set of western blot experiments verified mTOR overexpression in HCC, in which 8 (62%) paired tumor tissues showed increased expression of mTOR proteins (Figure 4). Moreover, the average mTOR expression level was higher for grade III HCC compared to grade II HCC tissues. Immunostaining for phospho-mTOR (Ser2448) revealed that phospho-mTOR positivity was not detected in DNs and grade I HCCs except for two positive cases (14%) in high-grade DNs. PhosphomTOR immunostaining showed a grade-dependent increase in which immunopositivity was detected in 4 (33%) of 12 grade II HCCs, 8(44%) of 18 grade III/IV HCCs, and 3 (75%) of 4 metastatic adenocarcinomas (Figure 3). Thus, phospho-mTOR expression showed HCC grade dependence with a significant difference in expression levels between grade I and grade II HCC tissues (P=0.05; Kruskal-Wallis rank sum test) (Table 1). Interestingly, the expression of phospho-mTOR showed a relatively strong correlation with LC3 expression ($R^2=0.56$; Pearson's correlation) in IHC intensitysum scores. On the other hand, phospho-mTOR immunostaining showed local expression (Figure 2) and a relatively weak correlation with Beclin1 expression $(R^2=0.38)$ and an even weaker correlation with mTOR expression ($R^2=0.29$; Pearson's correlation). Therefore, it is likely that the regulatory mechanisms leading to phosphorylation and activation of mTOR are at least partly separated from those that regulate mTOR expression itself.

Different Localization Pattern of Phospho-mTOR and LC3 Expression in Primary HCC and Metastatic Adenocarcinoma

Close examination of a typical phospho-mTORpositive HCC specimen revealed that phospho-mTOR protein was only focally expressed (Figure 2d). In the same field of tumor, an inverse pattern of staining for LC3 and phospho-mTOR was observed. Tumor cells with LC3 staining were negative for phospho-mTOR and the opposite was also found (Figure 2g and h). In other sets of HCC tissues that displayed both LC3positive cells and phospho-mTOR positive cells, the expression of these two proteins showed partly distinct localization, suggesting that proliferating cancerous cells markedly down-regulated the expression of autophagy protein LC3.

Discussion

In this study, evidence for increased Beclin1 and LC3 protein expression in high-grade HCC is provided. The immunohistochemical approach allowed examination of autophagy protein expression at the nontumor-tumor boundary as well as in relation to mTOR protein expression in different compartments of HCC specimens. These findings suggest that autophagy machinery activation frequently occurs in high-grade HCC.

Beclin1 overexpression has been reported in human brain tumors²⁴, gastric, colorectoral carcinoma²⁵, and HCC^{26,27}, although its relevance to tumor development was not clear. In a previous study of Beclin1 mRNA measurements in HCC, only one tumor sample showed more than a two-fold increase out of 27 paired tumor samples²⁷, indicating a lack of association with HCC. Another study that analyzed differentially expressed genes in HCC found that Beclin1 mRNA showed a significantly increased expression in five out of ten paired tumor samples²⁶. These differences can partly be reconciled in light of this study, as the majority of tissue samples used in the former study were grade I/II HCC tissues (17 out of 27), whereas the latter study used grade III HCC tissues. Here, Beclin1 overexpression was observed mostly in grade III/IV HCC, suggesting a role of Beclin1 in tumor development.

In this study, the overexpression of LC3 protein was observed in high-grade HCC. LC3 proform is cleaved into a soluble form known as LC3-I and further processed into a membrane-bound form, LC3-II, prior to incorporation onto the autophagosome membrane¹⁵. Although LC3-II is a very specific marker of the autophagosome/autolysosome, the steady-state levels of LC3-II may not accurately reflect cellular autophagic flux due to its rapid and dynamic regulation²⁸. There is a clear difference in terms of distribution between LC3-I and -II. The former was recovered exclusively in the supernatant, while the latter was found mostly in the pellet fraction. The cytosolic LC3 ratio (soluble LC3-II/LC3-I) reflected quantitative changes in proteolytic flux and was sensitively regulated by amino acids in rat hepatocytes and H4-II-E cells, more so than those of the total homogenate²⁰. However, the LC3 ratio of the total homogenate also showed a linear relationship to proteolytic flux. Concanavalin A treatment on hepatoma cell lines induced the formation of LC3-II as well as de novo synthesis of LC3-I mediated by the autophagic pathway²⁹. Similarly, overexpression of both LC3 isoforms and an increased LC3-II/LC3-I ratio in the total homogenates of HCC tissues were demonstrated in this study. Morphological and morphometric methods utilizing electron microscopy have been the most reliable method for monitoring autophagy³⁰. Autophagosome formation was confirmed in an LC3-positive specimen examined with transmission electron microscopy (EM). Thus, autophagosome formation in HCC was confirmed both by EM and by LC3 ratio measurements.

This study showed a grade-dependent increase of mTOR immunostaining in HCC tissues. Previous studies reported a decrease or absence of PTEN immunostaining in 43 of 105 HCC specimens³¹ and in 29 of 46 HCC specimens³², which indicates phosphatidylinositol 3-kinase/AKT/mTOR/S6K pathway activation in HCC. In another study, only a small fraction (5%) of HCC tissues showed increased expression of mTOR, whereas overexpression of phospho-mTOR was evident in 15% of HCC samples. Increased expression of S6K was found in 45% of cases, and phospho-mTOR overexpression was associated with increased total cytoplasmic S6K, which in turn is associated with the degree of tumor differentiation²². However, no association was found between S6K and mTOR expression and proliferation as measured by the Ki-67-labeling index. Another study found that the mTOR pathway was activated in 40% of 166 patients with HCC undergoing orthotopic liver transplantation²³. Interestingly, a study concerning the regulation of autophagy in the fat body of Drosophila melanogaster concluded that S6K is essential for autophagy and that the inhibition of autophagy by mTOR and the activation of S6K must be effected through different branches of the mTOR pathway³³. Thus, it is possible that the activation of both mTOR and S6K may have a positive effect on autophagy regulation depending on the cell type. Nevertheless, other factors not studied here may play a role in the regulation of autophagy in HCC, including other signal pathways and transcriptional regulation. For instance, the Ras/RAF1/MEK1/2/ ERK1/2 pathway promotes autophagy, and activation of Erk1/2stimulates GTPase-activation protein GAIP and abolishes the inhibitory effect of trimeric Gi3 protein on autophagy in human colon cancer HT-29 cells³⁴. Different localizations of phospho-mTOR and LC3 were observed in this study, suggesting that mTOR plays a negative regulatory role in autophagy³⁵. However, mTOR is not activated in a large portion of primary HCC and metastatic adenocarcinoma tissues that express autophagy protein LC3. A recent study demonstrated that autophagy is localized to the center of a transplanted epithelial tumor mass prior to the acquisition of a blood supply³⁶. Analogously, these data indicate heterogeneous tissue microenvironments and potential metabolic stresses in large portions of highgrade HCC and metastatic adenocarcinoma tissues, such as nutrient deprivation, hypoxia, and ischemia.

Programmed cell death can be divided into apoptotic (type I) and autophagic (type II) cell death. In addition, there may be forms of programmed necrosis as well as other death pathways that are less well defined³⁷. Previous studies have demonstrated that Beclin1-Vps34-mediated autophagy is negatively regulated by a proto-oncogene Bcl-2, providing a link to autophagy and apoptosis⁷. Partial silencing of Beclin1 aggravates doxorubicin- and Fas-induced apoptosis in HepG2 cells, indicating that blocking autophagy may sensitize cells to apoptotic stimuli³⁸. Moreover, mammalian cells under conditions of nutrient depletion as well as genetic or pharmacological inhibition of autophagy have been shown to undergo apoptotic death^{16,39}. Similarly, autophagy was found to be critical for the survival of cells with impaired apoptotic machinery: an ongoing autophagy process could support cell survival for several weeks following growth factor withdrawal during which growth factor readdition led to cell recovery⁴⁰. Given these interwoven cell death pathways, it is possible that autophagy may preserve cellular homeostasis while suppressing the latent apoptotic program in HCC.

Beclin1 functions as a platform for the formation of multi-component complexes involving Bcl-2, PI3KC3, and UVRAG⁴¹. Human vacuolar protein sorting 34 (Vps34) participates in the early stage of autophagosome formation as a Beclin1-Vps34 complex⁴² but also plays a role in multiple vesicular trafficking pathways including endocytosis, sorting of receptors in multivesicular endosomes, and transport of lysosomal enzymes from the trans-Golgi network (TGN) to endosomes and lysosomes⁴³. Tumor invasion and metastasis are associated with altered lysosomal trafficking and increased expression of cathepsins⁵. Cancer cells, particularly those at the invasive edges of tumors, often contain redistributed lysosome localizations from a perinuclear to a peripheral pattern. The lysosomal contents secreted into the extracellular space including cathepsins may participate in degrading the extracellular matrix, thereby increasing cellular motility, invasion and angiogenesis. However, it has not been addressed whether and how autophagy might alter tumor metastasis³⁷. Understanding the role of autophagy regulatory genes in vesicle trafficking can potentially shed light on the metastatic potential of tumors.

At this time, it is not clear whether autophagy acts as a tumor suppressor or protects cancer cells from metabolic and drug-induced stresses. During the evolution of a tumor, the autophagy process might have tumor promoting and inhibiting properties at different times and in different contexts. Autophagy is localized to the center of a transplanted epithelial tumor mass prior to the acquisition of a blood supply³⁶ and also plays a pivotal role in the survival of colorectoral cancer cells that have acquired austerity¹⁶. In light of these findings, if autophagy usually contributes to cell survival in liver cancer, inhibition of the autophagy process may result in decreased tolerance and serve as a new strategy for inducing tumor cell death. In such a case, it is possible that autophagy inhibitors such as bafilomycin A1 or siRNAs specific for autophagyrelated genes together with anti-cancer drugs would improve the efficacy of liver cancer therapy.

Conclusions

The results of this study demonstrate that autophagy proteins are upregulated and that autophagy is activated in high-grade HCC tissues. The autophagy-specific gene Beclin1 is overexpressed in high-grade HCC and in metastatic adenocarcinoma. Furthermore, autophagosome membrane-bound protein LC3-II is overexpressed in HCC, and increased autophagosome formation can be confirmed by EM. Interestingly, although the expression of mTOR was increased and a strong correlation with Beclin1 expression was observed, phospho-mTOR showed focal expression pattern that was distinct from LC3 expression in HCC tissues. These data suggest that the autophagy machinery could be relevant to the progression of HCC and that regulation of the autophagy process may have diagnostic and therapeutic potential.

Materials and Methods

Tissue Specimens

Subjects consisted of 74 patients who underwent surgical removal of liver cancer at the Samsung Medical Center (Seoul, Korea) from 2007 to 2008. All patients agreed to enroll in the study and each gave informed consent. The institutional review board of Samsung Medical Center approved all protocols regarding the patients' agreement. From 8 patients, both frozen HCC tissues and FFPE specimens were obtained (3 grade II and 5 grade III HCCs). The 69 FFPE specimens used in the present study consist of 12 lowgrade DNs, 14 high-grade DNs, 9 grade I, 12 grade II, 15 grade III, 3 grade IV cancers by Edmondson's classification⁴⁴, and 4 metastatic adenocarcinoma tissues including paired nonneoplastic liver tissues. The 13 quick-frozen and -70°C stored HCC tissues used in the western blotting consist of 3 grade II and 10 grade III cancers by Edmondson's classification⁴⁴.

Immunohistochemistry

Immunostaining was performed on routinely processed, formalin-fixed, paraffin-embedded sections using a standard avidin-biotin peroxidase technique after antigen retrieval in a microwave oven. The primary antibodies included phospho-mTOR (Ser2448) (49F9, 1 : 50; Cell Signaling Technology, Danvers, MA, USA), LC3 (MAP1LC3B) (polyclonal, 1:100; Abgent, San Diego, California, USA), BECN1 (Beclin1) (polyclonal, 1:135; Santa Cruz Biotechnology, Santa Cruz, California, USA), and mTOR (7C10, 1:40; Cell Signaling Technology). After deparaffinization and rehydration, 4-µm thick sections on silane-coated slides were heat-pretreated in a citrate buffer (pH 6.0) for BECN1 or in a TE buffer (pH 9.0) for p-mTOR, LC3 (MAP1LC3B), and mTOR. The avidin-biotin technique was applied using DAB for visualization and hematoxylin for nuclear counterstaining. Prostate adenocarcinoma tissues and colon cancer tissues served as positive controls for mTOR, p-mTOR, and LC3 antibodies^{16,22}. Beclin1 immunostaining was performed according to the manufacturer's protocols.

Interpretation of Immunoexpression

The IHC data for 69 FFPE samples and 4 markers were obtained, each of which is featured with the intensity, the proportion and cellular localization of their expression. Cases with 5% or more of tumor cells staining positive were scored as positive. All markers showed negative staining in noncancerous tissues. Immunoreactivity was assessed according to intensity (weak, moderate, and strong) and area proportion (%). The intensity score was graded 0 for absence of staining, 1 for weak staining, 2 for moderate staining, and 3 for strong staining. The proportion score was measured as the percent of tissue type showing a given intensity score. The intensity-sum score was calculated by multiplying the intensity score by the proportion score. The intensity and prevalence of each antibody was scored independently and scores were corroborated by two specialized pathologists.

Electron Microscopy

The fresh HCC specimens were obtained from liver cancer patients and a tissue slice with a thickness of 1 mm was cut with a blade. The slices were immersed in 2.5% glutaraldehyde in 0.1 mol/L sodium phosphate buffer (pH 7.4) overnight at 4°C. The samples were then post-fixed with 1.0% OsO_4 and dehydrated in graded ethyl alcohol. After complete dehydration, samples were infiltrated with propylene oxide, embedded in Epok812, and sectioned. The ultra-thin sections were then stained with uranyl acetate and lead citrate and were evaluated using a Hitachi 7100 transmission

electron microscope.

Western Blot

Cellular protein was extracted from 13 frozen tissues using a Tissue Extraction Reagents II kit (Biosource International, Camarillo, CA, USA), and protein concentration was determined by a Bradford assay. Twentyfive micrograms of total cell lysates were separated by 8-10% Tris-glycine SDS-PAGE and were then transferred to a polyvinylidene difluoride membrane. Membranes were blocked with TBS containing 5% (w/v)skim milk with 0.05% Tween 20, washed with TBS containing 0.05% Tween 20 (TBST) and were then incubated overnight at 4°C with primary antibody. The primary antibodies included LC3 (MAP1LC3B) (polyclonal, 1:500; Cell Signaling Technology), BECN1 (polyclonal, 1:500; Santa Cruz Biotechnology), and mTOR (7C10, 1:500; Cell Signaling Technology). After washing in TBST, membranes were incubated for 1 h at 4°C with horseradish peroxidase-conjugated goat anti-rabbit IgG antibody (1:15000; Zymed Laboratories, South San Francisco, California, USA). Signals were detected using enhanced chemiluminescence detection reagents (Millipore, Billerica, MA, USA). In order to ascertain the loading amount of proteins and the efficiency of transfer, the transferred membrane was stained with Coomassie brilliant blue. The density of each band was measured using Progenesis Samespots software (Nonlinear Dynamics, New Castle, UK).

Statistical Analysis

Statistical analyses were applied for the interpretation of IHC and western blot data using the R statistical packages. The correlations between pairs of markers were measured by Pearson's correlation (R^2). The statistical significance of differences in value distribution between adjacent cancer grades was determined by Kruskal-Wallis rank sum test. Outliers in the replicated western blot data were detected and removed using the Grubb's test implemented in the R package, outliers.

Acknowledgements

This work was supported by intramural research funds of CbsBioscience, Inc (CBS-08-71).

References

- Levine, B. Eating oneself and uninvited guests: autophagy-related pathways in cellular defense. *Cell* 120, 159-162 (2005).
- 2. Edinger, A.L. & Thompson, C.B. Death by design:

apoptosis, necrosis and autophagy. *Curr. Opin. Cell Biol.* **16**, 663-669 (2004).

- 3. Hay, N. & Sonenberg, N. Upstream and downstream of mTOR. *Genes Dev.* **18**, 1926-1945 (2004).
- Mamane, Y., Petroulakis, E., LeBacquer, O. & Sonenberg, N. mTOR, translation initiation and cancer. *Oncogene* 25, 6416-6422 (2006).
- Kroemer, G. & Jäättelä, M. Lysosomes and autophagy in cell death control. *Nat. Rev. Cancer* 5, 886-897 (2005).
- Liang, X.H. *et al.* Protection against fatal sindbis virus encephalitis by Beclin, a novel Bcl-2-interacting protein. *J. Virol.* 72, 8586-8596 (1998).
- Liang, X.H. *et al.* Induction of autophagy and inhibition of tumorigenesis by Beclin 1. *Nature* 402, 672-676 (1999).
- 8. Qu, X. *et al.* Promotion of tumorigenesis by heterozygous disruption of the Beclin 1 autophagy gene. *J. Clin. Invest.* **112**, 1809-1820 (2003).
- Yue, Z. *et al.* Beclin 1, an autophagy gene essential for early embryonic development, is a haploinsufficient tumor suppressor. *Proc. Natl. Acad. Sci. USA* 100, 15077-15082 (2003).
- Aita, V.M. *et al.* Cloning and genomic organization of Beclin 1, a candidate tumor suppressor gene on chromosome 17q21. *Genomics* 59, 59-65 (1999).
- Høyer-Hansen, M. *et al.* Vitamin D analog EB1089 triggers dramatic lysosomal changes and Beclin 1mediated autophagic cell death. *Cell Death Differ.* 12, 1297-1309 (2005).
- Izuishi, K. *et al.* Remarkable tolerance of tumor cells to nutrient deprivation: possible new biochemical target for cancer therapy. *Cancer Res.* 60, 6201-6207 (2000).
- Kitano, M. *et al.* Dynamic imaging of pancreatic diseases by contrast enhanced coded phase inversion harmonic ultrasonography. *Gut* 53, 854-859 (2004).
- Levine, B. Cell biology: Autophagy and cancer. *Nature* 446, 745-747 (2007).
- Kabeya, Y. *et al.* LC3, a mammalian homologue of yeast Apg8p, is localized in autophagosome membranes after processing. *EMBO J.* **19**, 5720-5728 (2000).
- Sato, K. *et al.* Autophagy is activated in colorectal cancer cells and contributes to the tolerance to nutrient deprivation. *Cancer Res.* 67, 9677-9684 (2007).
- Ogier-Denis, E. & Codogno, P. Autophagy: a barrier or an adaptive response to cancer. *Biochim. Biophys. Acta. (BBA)-Reviews on Cancer* 1603, 113-128 (2003).
- Alva, A.S., Gultekin, S.H. & Baehrecke, E.H. Autophagy in human tumors: cell survival or death? *Cell Death Differ*. 11, 1046-1048 (2004).
- Mizushima, N. & Yoshimori, T. How to interpret LC3 immunoblotting. *Autophagy* 3, 542-545 (2007).
- Karim, M.R. *et al.* Cytosolic LC3 ratio as a sensitive index of macroautophagy in isolated rat hepatocytes and H4-II-E cells. *Autophagy* 3, 553-560 (2007).
- 21. Easton, J.B. & Houghton, P.J. mTOR and cancer

therapy. Oncogene 25, 6436-6446 (2006).

- Sahin, F. *et al.* mTOR and P70 S6 kinase expression in primary liver neoplasms. *Clin. Cancer Res.* 10, 8421-8425 (2004).
- Sieghart, W. *et al.* Mammalian target of rapamycin pathway activity in hepatocellular carcinomas of patients undergoing liver transplantation. *Transplantation* 83, 425-432 (2007).
- Miracco, C. *et al.* Protein and mRNA expression of autophagy gene Beclin 1 in human brain tumours. *Int. J. Oncol.* **30**, 429-436 (2007).
- 25. Lee, J.W. *et al.* Somatic mutations of BECN1, an autophagy-related gene, in human cancers. *APMIS*. **115**, 750-756 (2007).
- 26. Song, H. *et al.* Genes encoding Pir51, Beclin 1, RbAp48 and aldolase b are up or down-regulated in human primary hepatocellular carcinoma. *World J. Gastroenterol.* **10**, 509-513 (2004).
- Daniel, F. *et al.* Beclin 1 mRNA strongly correlates with Bcl-XL mRNA expression in human hepatocellular carcinoma. *Cancer Invest.* 25, 226-231 (2007).
- Tanida, I., Minematsu-Ikeguchi, N., Ueno, T. & Kominami, E. Lysosomal turnover, but not a cellular level, of endogenous LC3 is a marker for autophagy. *Autophagy* 1, 84-91 (2005).
- 29. Chang, C.-P. *et al.* Concanavalin A induces autophagy in hepatoma cells and has a therapeutic effect in a murine in situ hepatoma model. *Hepatology* **45**, 286-296 (2007).
- Mizushima, N. Methods for monitoring autophagy. Int. J. Biochem. Cell Biol. 36, 2491-2502 (2004).
- Hu, T.-H. *et al.* Expression and prognostic role of tumor suppressor gene PTEN/MMAC1/TEP1 in hepatocellular carcinoma. *Cancer* 97, 1929-1940 (2003).
- 32. Rahman, M.A. *et al.* Impact of PTEN expression on the outcome of hepatitis C virus-positive cirrhotic hepatocellular carcinoma patients: Possible relationship with COX II and inducible nitric oxide synthase. *Int. J. Cancer* 100, 152-157 (2002).

- Scott, R.C., Schuldiner, O. & Neufeld, T.P. Role and regulation of starvation-induced autophagy in the drosophila fat body. *Dev. Cell* 7, 167-178 (2004).
- Meijer, A.J. & Codogno, P. Regulation and role of autophagy in mammalian cells. *Int. J. Biochem. Cell Biol.* 36, 2445-2462 (2004).
- Codogno, P. & Meijer, A.J. Autophagy and signaling: their role in cell survival and cell death. *Cell Death Differ.* 12, 1509-1518 (2005).
- Degenhardt, K. *et al.* Autophagy promotes tumor cell survival and restricts necrosis, inflammation, and tumorigenesis. *Cancer Cell* 10, 51-64 (2006).
- Hippert, M.M., O'Toole, P.S. & Thorburn, A. Autophagy in Cancer: Good, Bad, or Both? *Cancer Res.* 66, 9349-9351 (2006).
- Daniel, F. *et al.* Partial Beclin 1 silencing aggravates doxorubicin- and Fas-induced apoptosis in HepG2 cells. *World J. Gastroenterol.* 12, 2895-2900 (2006).
- 39. Boya, P. *et al.* Inhibition of macroautophagy triggers apoptosis. *Mol. Cell Biol.* **25**, 1025-1040 (2005).
- 40. Lum, J.J. *et al.* Growth factor regulation of autophagy and cell survival in the absence of apoptosis. *Cell* **120**, 237-248 (2005).
- Liang, C. *et al.* Autophagic and tumour suppressor activity of a novel Beclin1-binding protein UVRAG. *Nat. Cell Biol.* 8, 688-698 (2006).
- Kihara, A., Kabeya, Y., Ohsumi, Y. & Yoshimori, T. Beclin-phosphatidylinositol 3-kinase complex functions at the trans-Golgi network. *EMBO Rep.* 2, 330-335 (2001).
- 43. Zeng, X., Overmeyer, J.H. & Maltese, W.A. Functional specificity of the mammalian Beclin-Vps34 PI 3kinase complex in macroautophagy versus endocytosis and lysosomal enzyme trafficking. *J. Cell Sci.* **119**, 259-270 (2006).
- Edmondson, H. & Steiner, P. Primary carcinoma of the liver: a study of 100 cases among 48,900 necropsies. *Cancer* 7, 462-503 (1954).